TÜBİTAK

Turkish Journal of Physics

http://journals.tubitak.gov.tr/physics/

Research Article

Turk J Phys
(2013) 37: 39 – 48

doi:10.3906/fiz-1201-11

One proton emission with structural effects in medium mass nuclei

Chandrasekaran Anu RADHA*, Velayudham RAMASUBRAMANIAN
School of Advanced Sciences, VIT University, Vellore-632014, Tamil Nadu, India

Received: 26.01.2012 • **Accepted:** 02.05.2012 • **Published Online:** 20.03.2013 • **Printed:** 22.04.2013

Abstract: In this work proton emission from deformed nuclei is discussed with the quadrupole deformation values. The deformation is investigated using potential energy surface plots. The identified proton emitters are found to have odd Z since the unpaired proton is less bound, and they are readily available for emission. Using the exotic decay model to the medium mass nuclei, the new proton emitters are analyzed with the inclusion of centrifugal barrier. The proton decay half-lives are calculated and compared with literature values. A discussion pertaining to single proton emission with structural effect will be a pivotal point in our study.

Key words: Proton emission, quadrupole deformation, potential energy surface

1. Introduction

Proton radioactivity offers a definite probability for wealthy information about the nucleus located beyond the proton drip line. The simplicity of the decay process has encouraged researchers to hold proton radioactivity as an important probe into nuclear physics [1, 2]. Generally beta decay is allowed even for small differences in binding energies of parent and daughter nuclei. Gamma emission occurs if the beta decay leaves the daughter nucleus in the excited state [3]. Beta delayed emission of a single proton, diproton or one or more neutrons has become a subject of interest in recent years [4]. The high repulsive Coulomb force pushes the line of minimum energy closer to the valley of stability in the case of proton emission which is insignificant in the neutron rich side [5]. The nucleus is a many body system in which the residual interaction affects the decay properties [6]. Due to the strong energy dependence, the conversion of the branching ratio into the corresponding matrix element is energy dependent [7]. Proton decay studies help in knowing the structural information of the emitting nucleus because the proton decay rate varies depending on the orbital angular momentum of the emitted proton [8, 9]. This is due to the lower mass of the proton when compared to an alpha particle. In proton emission increase of centrifugal barrier is observed because of the non vanishing angular momentum carried by the proton [10, 11].

To directly study the ground state proton emitters, however, one must look at nuclei with half-lives in the range 1 μs to 1 s, to which current experimental capabilities are geared to handle. This has made investigators look at heavier elements with $Z > 50$ [12]. The description of the theoretical framework that is used to identify the proton emitters is given involving a separation-energy calculation. Exotic decay model [13–16] is used to calculate the half-life of the known proton emitters. Then the theoretical formalism of the microscopic model, namely, the Triaxially Deformed Cranked Nilsson Strutinsky Shell Correction method [17, 18] is given. This model gives the role of normal and quadrupole deformations observed in the possible proton emitters. The

*Correspondence: canuradha@vit.ac.in

novel idea used here is plotting the *Potential Energy Surfaces* (PES) for the shape calculations in the possible proton emitters.

2. Theoretical formalism for single proton radioactivity

In this work, separation energies are calculated for different proton numbers Z for various isotones and different neutron numbers for various isotopes. The mass excess for the parent, daughter and emitted nuclei are taken from the Audi Wapstra mass table [19]. Separation energies are calculated for different proton numbers Z for fixed values of $N = \{3, 6, 8, 10, 11, 12, 14, 16, 18, 20, 22\ldots\}$ and different Z for various fixed N values. The separation energy is calculated using the relation

$$S_p(Z,N) = -M(Z,N) + (Z-1,N) + m_p. \tag{1}$$

It has been known for a long time that single particle separation energies are valuable tools to extract systematic trends over the chart of the nuclei [20]. Figure 1 shows the variation of one proton separation energy as a function of neutron number (S_p vs. N) for different isotopes and Figure 2 shows the variation of one proton separation energy as a function of proton number (S_p vs. Z) for different isotones. The probable one proton emitters are identified from their separation energy values since the one proton emitters should have S_p value < 0. From Figures 1 and 2 it is found that the nuclei like Sc^{39}, Sb^{105}, I^{109}, I^{111},$Cs^{112,115}$, $La^{117,119}$, $Pr^{121,122,123}$, $Pm^{126,127}$, Eu ^{130,131,132,133}, $Tb^{136,137,138,139}$, $Ho^{140,141}$ and $Tm^{146,147}$ having $S_p < 0$, showing that they are efficient single proton emitters. Here Sc^{39} has not been observed in the Be^9 (Ni^{58}, X) reaction, and so should decay 100% by proton emission, with a half-life shorter than 300 ns [21]. For instance, as of this writing, I^{111}, Cs^{115}, La^{119}, Pr^{122}, Pr^{123}, Pm^{126}, Pm^{127}, Eu^{132}, Eu^{133} and $Tb^{136,137,138,139}$ have not been found in experiment and the above nuclei are predicted theoretically as probable proton emitters.

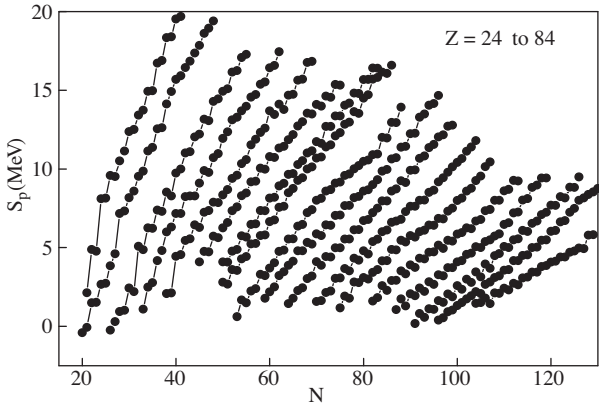

Figure 1. One proton separation energy as a function of neutron number for different isotopes ($Z = 24$ to 84).

3. Half-life calculations using exotic decay model – SK model

The half lives of proton radioactivity are studied using the SK (Shanmugam-Kamalaharan) model. A finite range Yukawa plus exponential potential along with the Coulomb potential is used for the post scission region and a third order polynomial is used for the overlapping region. While the centrifugal barrier has negligible role to play in cluster radioactivity, it becomes appreciable in the case of alpha decay. For proton emission the

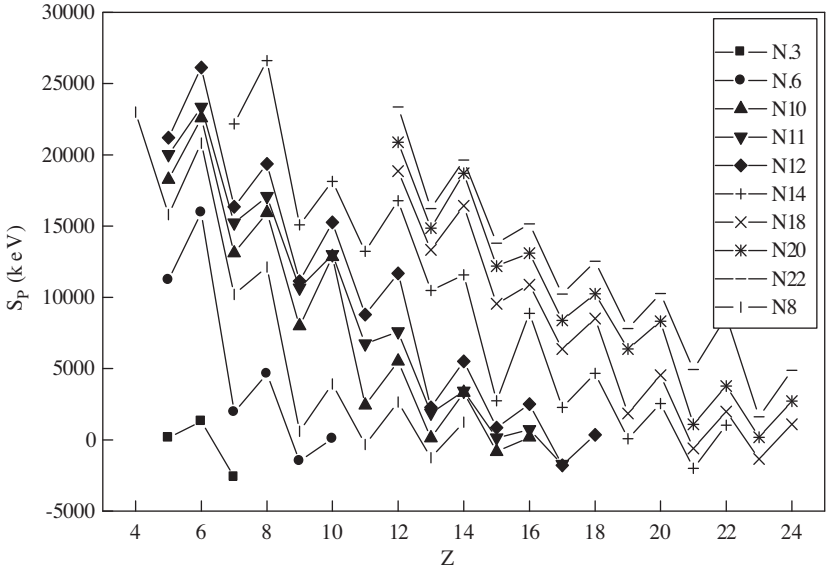

Figure 2. One proton separation energy as a function of proton number Z for different isotones (N = 3 to 22).

centrifugal effect should become very much considerable; hence a centrifugal barrier is added to the post scission region for considering proton radioactivity. Here, the parent is considered to be deformed and so to include the deformation effects spheroidal deformation β_2 and Nilsson's hexadecapole deformation β_4 are considered. The half-life of the meta-stable system is

$$T = \frac{\ln 2}{\nu P}, \tag{2}$$

where

$$v = \frac{\omega}{2\pi} = \frac{E_v}{h} \tag{3}$$

denotes the number of assaults on the barrier per second. The zero point vibration energy is given by

$$E_v = \frac{\frac{\pi\hbar}{2}\left[\frac{2Q}{\mu}\right]^{1/2}}{C_1 + C_2}, \tag{4}$$

where C_1 and C_2 are the "central" radii of the fragments given by

$$C_i = 1.18A_i^{1/3} - 0.48, \quad i = 1, 2,$$

and μ is the reduced mass the system.

The probability per unit time of penetration P through the barrier is

$$P = \frac{1}{1 + e^K}, \tag{5}$$

where K is the action integral.

Proton radioactivity is an excellent platform to study quantum mechanical tunneling through a potential barrier. The rate of proton emission is related the proton's capability to tunnel through the barrier produced

by the nuclear, Coulomb and centrifugal potentials. Orbital angular momentum in deformed nuclei cannot give the complete information because the high penetrability, low value of the orbital angular momentum component could have predominant effect over the decay width, even for a small value of the amplitude. During proton emission, the proton has to tunnel through the nuclear potential to escape from the parent nucleus. If spin and parity of the initial and final nuclear states were known, then the angular momentum of the emitted proton would also be calculated [22]. Hence the proton has an expected angular distribution relative to the spin axis of the emitting nucleus. This could be related to the time it takes for the proton to penetrate the potential barrier that is the tunneling time. Proton emission half-lives depend mainly on the proton separation energy and orbital angular momentum, but it is not depending on the intrinsic structure of proton emitters, e.g., on the proton-core potential [23, 24]. This emphasizes that the lifetimes of deformed proton emitters will provide information on the angular momentum of the nucleus concerned and so its structural information can be obtained thereafter [25, 26].

4. Deformation studies in single proton emitters

The deformation in the ground state of proton emitters can be and is studied here using a deformed shell model called the *cranked Nilsson model with Strutinsky shell correction method* [17, 18]. Quadrupole moments vary systematically with proton and neutron numbers. Nuclei with magic number configuration are spherical and have zero quadrupole moment. In the Nilsson model, the potential in Hamiltonian comprises the anisotropic harmonic oscillator potential plus the spin-orbit and centrifugal potentials. The zero temperature potential energy surfaces for single proton emitters have been obtained by the tuned Strutinsky procedure.

The calculation performed here assumes *ground state spin*, without temperature (0.0 MeV), with γ from -180° to -120° in steps of 10°, and β from 0.0 to 0.8 in steps of 0.01. The Hill Wheeler expressions for the frequencies have been used in the cranked Nilsson model.

The calculations are carried out by varying values of ω in steps of $0.01\omega_0$ from $\omega = 0$ to $0.15\omega_0$, ω_0 being the oscillator frequency. Since the work is focused on non-collective oblate (γ = -180°) and collective prolate (γ = -120°) shapes, γ is varied from -180° to -120° in steps of 10°. The β values are varied from 0 to 0.8 in steps of 0.01. Obtaining potential energy surfaces of the considered nuclei as a function of deformation β and non-axial γ parameters at ground state spin helps to identify the structure of the parent as well the daughter nuclei. By minimizing the free energy with respect to β and γ (deformation parameters) at constant spin and temperature the potential energy surfaces for the nuclei can be constructed and shape transitions can be detected. PES is the three dimensional contour plot having plane polar co-ordinates, $\beta\cos\gamma$ along the x-axis and $\beta\sin\gamma$ along the y-axis with corresponding energy values. The resulting energy values are normalized according to triaxially deformed cranked Nilsson Strutinsky method with shell correction prescription and then minimum at fixed spin over different deformations is searched for [27]. Deformed shape is nothing but the deviation from spherical shape of a nucleus. A liquid drop takes a spherical shape maintaining minimum potential energy value with small surface area to volume ratio [28, 29]. Any deformation from the spherical shape is because of the competition between the Coulombic and surface energies. Coulombic force repels the protons to stay far and favors deformation since the Coulombic force is not so strong to increase the nuclear volume and create more surfaces among the protons. This increases the surface energy by increasing the surface area. The surface tension force balances the Coulombic force to keep the surface area a minimum. The surface energy tries to preserve the spherical shape. This surface energy domination is found in light nuclei making them spherical. As Z increases, the Coulombic repulsion increases favoring deformation [30].

As Z increases, the number of valence nucleons outside the closed shell increases. This decreases the vibration energy as they become less compact. But the interaction between the valence nucleons and closed core brings about slight deformation. For nuclei which are not far from stability line, this is the case. For nuclei, far from stability, significant shape deformation in their ground state is observed. This is reflected in the calculations of quadrupole deformation parameter. It also gives the theoretical framework for obtaining potential energy surfaces of the considered nuclei as a function of deformation β and nonaxial γ parameters at different spins by the Strutinsky shell correction method.

Our calculated deformation values are compared with the values of Moller [31] and it is found that our values are in agreement with their values. For Sc^{39}, the nucleus is normally deformed. Moderate deformation is observed for $62 < Z < 67$. The variations in the calculated values of γ when compared with Moller calculations are found to be negligibly small. Both oblate and prolate quadrupole deformed shapes are observed in the chosen region. The potential energy surfaces for the nuclei are constructed to confirm the structural change and shape transitions exhibited by the proton emitters.

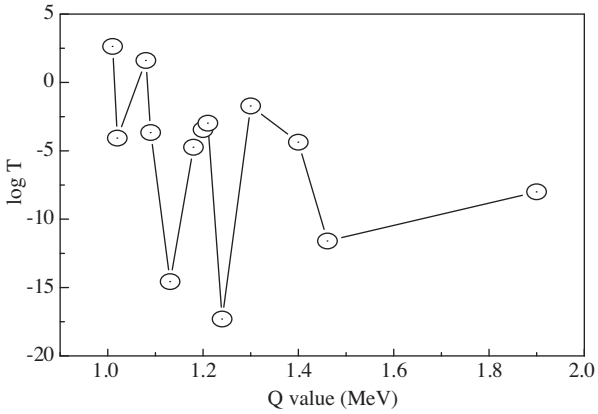

Figure 3. Variation of half-life as a function of Q value for the medium mass proton emitters.

5. Results and discussion

The half-life of proton decay strongly depends on the energy of the proton, that is, the Q-value of the reaction. As the value of Q changes, the half-life changes from 10^{10} s to 10^{-12} s and are clearly visible in Figure 3. This shows the strong dependence of the lifetime on Q falling with a small change in Q-value. It obviously shows that the ground state emission will not be observed immediately above the drip line because when Q is less the half-life is dominated by β^+ decay. For small values of Q, proton emission half-lives are very long and the total decay is dominated by beta decay. The Q-value which gives rise to proton emission increases with increase in nuclear charge. For light nuclei it is found to be 0.5 MeV and for heavy nuclei it nears 2 MeV.

Beyond $Z = 83$, no one-proton emitter is identified as the nuclides are prone to fission or alpha decay [32–34]. For heavier nuclei, several proton emitters are found to exist for the same element. The variation of Q as a function of atomic number Z is shown in Figure 4. It is found that for light nuclei, no one-proton emitters are identified. The region $Z = 35$ to 50 is a gap in the figure showing that this region is fertile for diproton emission. As the atomic number increases, the Q value increases showing the enhanced emission of one-proton from those parent nuclei (see Figure 3).

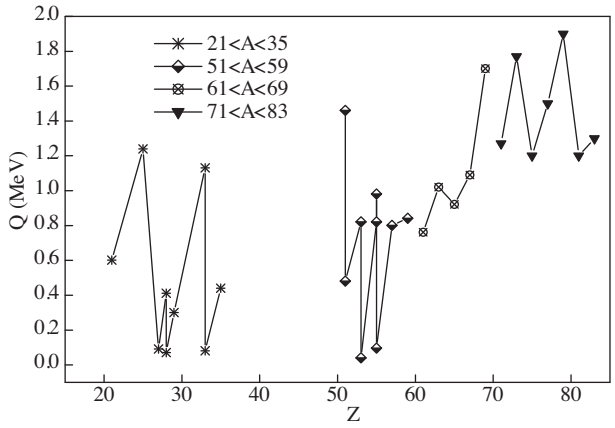

Figure 4. Plot of Q of the one proton emission as a function of Z.

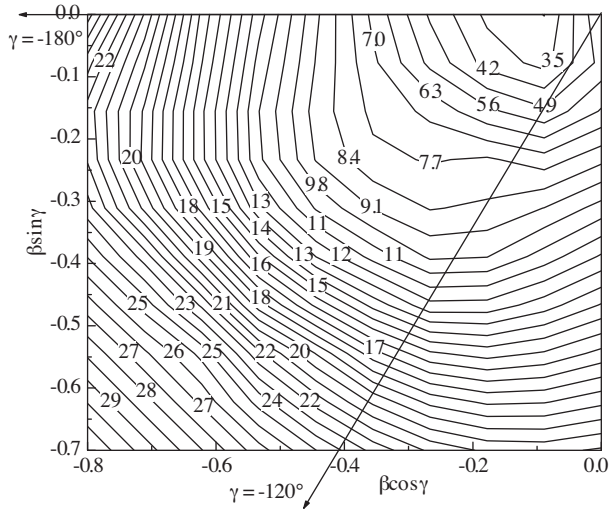

Figure 5. Prolate shape determination by Potential Energy Surface for Sc^{39}.

Half-lives for proton emissions depend exponentially on the energy and almost linearly on the angular momentum (almost one order of magnitude for each unit of angular momentum). To find the effect of deformation on proton emitters, PES graphs are a powerful tool to study the shape of the selected nucleus. Figure 6 shows the potential energy surface for Tb^{138} ($N \neq Z$ case) at the ground state spin of $1\hbar$ having zero temperature. The minimum lies in the prolate region, confirming that Tb^{138} is prolate shape with normal deformation. Significant deformation is obtained from Figure 7 in the odd Z nucleus of Ho^{141} using the cranking model matches the β values as 0.286 concludes the triaxial shape in its ground state. While calculating the half-lives of Holmium isotopes, $Ho^{140,141}$ are more deformed ($\beta \sim 0.286$) when compared with other Holmium isotopes $Ho^{142,143,145}$. The former are found to have shorter half-lives than the other isotopes, confirming that deformation enables effective proton emission. Competing minima are found to occur along non-collective oblate

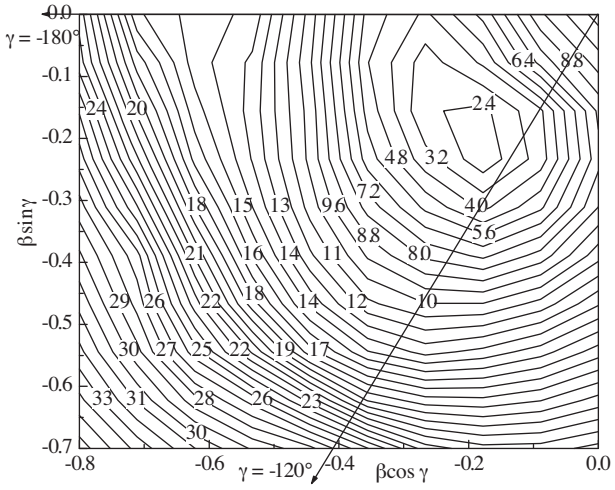

Figure 6. Prolate shape determination by Potential Energy Surface for Tb^{138}.

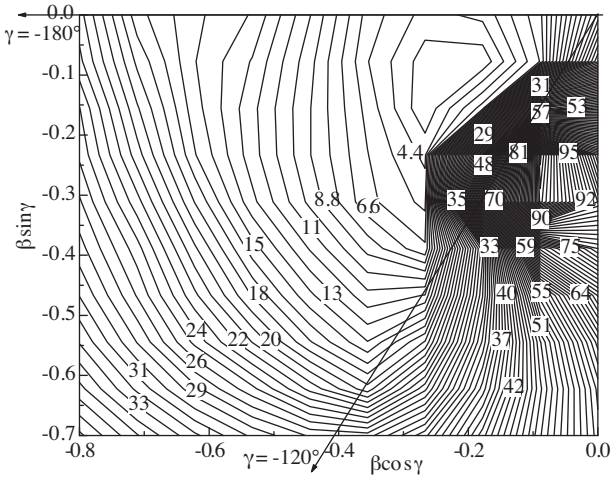

Figure 7. Triaxial shape determination by Potential Energy Surface for parent Ho^{141}.

Table 1. Calculated quadrupole deformation values in comparison with Moller values.

Nucleus	Calculated quadrupole deformation values	Moller quadrupole deformation values [31]
Sc^{39}	0.022	0
Sb^{105}	0.082	0.081
I^{109}	0.152	0.16
Cs^{112}	0.222	0.208
Cs^{113}	0.183	0.207
La^{117}	0.251	0.290
Eu^{130}	0.330	0.331
Eu^{131}	0.327	0.331
Tb^{138}	0.205	0.217
Tb^{139}	0.215	0.216
Ho^{140}	0.275	0.297
Ho^{141}	0.28	0.286
Tm^{145}	0.225	0.249
Tm^{146}	-0.159	-0.199
Lu^{150}	-0.11	-0.164
Lu^{151}	-0.05	-0.156
Ta^{156}	-0.01	-0.053
Re^{160}	0.05	0.080
Ir^{164}	0.05	0.089
Ir^{167}	0.15	0.116
Ir^{169}	0.143	0.134
Au^{169}	-0.05	-0.087
Au^{170}	-0.05	-0.096
Au^{171}	-0.065	-0.105
Au^{172}	-0.1	-0.105
Au^{173}	-0.052	-0.105
Au^{174}	-0.057	-0.122
Au^{175}	-0.1	-0.122
Tl^{176}	0.045	-0.053
Tl^{177}	-0.045	-0.053
Tl^{178}	-0.042	-0.053
Tl^{179}	-0.041	-0.053
Tl^{180}	-0.052	-0.053
Tl^{181}	-0.042	-0.053
Tl^{182}	-0.05	-0.053
Bi^{184}	0.05	0
Bi^{185}	-0.05	0
Bi^{186}	-0.04	0
Bi^{187}	0.01	0.001
Bi^{188}	0.01	0.002
Bi^{189}	0.02	0.003

and collective prolate lines. For ground state spins, the competition between collective oblate and non-collective oblate states is significant, which may cause rotational isomers. Proton emission from Ho^{141} and Eu^{131} has recently been observed at the Fragment Mass Analyzer [32, 33] and the decay rates cannot be explained by spherical WKB calculations. These nuclei are predicted to be highly deformed ($\sim$ 0.3). The observation of these and other proton emitters expected to be found in the $57 < Z < 65$ region should greatly increase our understanding of the role of deformation in the proton decay process. The calculated ground state quadrupole deformation of the nuclei in $56 < Z < 83$ is shown in Table 1. Odd Z are found to be good proton emitters and much deformed than their even Z neighbours. This is due to the reason that pairing correlations are strongly reduced in odd Z nuclei and as a result the nucleus is driven towards larger deformation. Much stronger pairing in even Z nuclei results in almost spherical shapes and the pairing energy prevents them from being proton emitters.

These deformation studies on proton emitters offer insight into proton binding and the evolution of shell structure at the edge of the stability line. A chain of proton emitting nuclei from $Z = 63$ to Z = 83 is established. Ho^{141} is found to have a triaxial shape. It is also reported by Davids [9]. The triaxiality is clearly indicated in the PES plot, Figure 7. Likewise, Lu^{151} is deformed and found to possess oblate structure with quadrupole deformation β = -0.156. Ferreira and Maglione [26] reported the same nucleus to be deformed with -0.18 $< \beta <$ -0.14.

Ta isotopes are found to be nearly spherical with $\beta = 0.045$. A similar analysis is given by Lalazissis et al. [25]. This may be due to the neutron number approaching the magic number 82. Table 2 shows the calculated half-lives on comparison with experimental and theoretical half-lives for Ho isotopes. It is found that the SK model used in calculating the half-lives gives values in agreement with the compared values. Using the effective liquid drop model Guzman [34] has calculated the half-lives of various proton emitters. There (using the effective liquid drop model) the angular momentum (ℓ) values for the proton decay of Ta^{156}, Re^{161} and Au^{171} are chosen in such a way as to give the best agreement between calculated and measured half-life values, but are not the ones suggested in the experimental literature.

Table 2. Calculated Half-life of Ho isotopes.

Nucleus	Quadrupole deformation	Calculated Half-Life (s)	Reference Half-Life (s)
Ho^{140}	0.275	1.07×10^{-4}	1.156×10^{-4} [37]
Ho^{141}	0.28	18×10^{-6}	11×10^{-6} [37]
Ho^{142}	0.23	2.31	2.187 [34]

In the present work we have taken $\ell = 2$ for all the selected nuclei and hence there is a mismatch in the half-lives of few emitters discussed in the table as those nuclei are assigned values $\ell = 0, 2, 5, 7$ in experimental calculations. Since the proton is a point charge, the effect of centrifugal potential is important. By comparing the deformation and the half-lives of the isotopes of different proton emitters, it may be considered that the maximum deformed nucleus is found to have a short half-life. For example, Ho^{141} has the maximum deformation among all the isotopes of Ho. It is found to have the least half-life of 18 μs. This value agrees with the reported value of 11 μs by Rykaczewski et al. [35] and 14 μs by Barmore et al. [36]. The difference in 1 or 2 units of angular momentum (ℓ) yields a difference of one or two orders of magnitude in the half-life.

Tm^{145} is found to have a prolate shape and the same was reported by Blank et al. [1] with $\beta = 0.23$. The present calculation predicts a slow change in shape from prolate to oblate for the Tm isotopes. The calculated half-life values of $Ho^{140,141}$ are quite agreeable with the values reported by Delion et al. [37].

The respective β and γ values for a particular nucleus can be easily identified using trigonometric calculations. The potential energy surface graphs declare the effect of shape occurrence in the ground state parent and daughter nuclei. The sensitivity of the calculated half-life upon angular momentum and quadrupole deformation play a significant role which allows proton emission to be a powerful tool to uncover triaxial shapes in nuclei.

6. Conclusion

Using the calculated separation energy values, new one-proton emitters are identified. The region $50 < Z < 83$ in the periodic table is found to be a fertile region for one-proton emission. The differences in deformation between the isotopes are very small and it is one of the causes for changes in half-lives. Most of the nuclei are found to have a modest non-zero quadrupole deformation in the chosen medium mass region and it indicates the role of deformation in the proton emitters. Modest deformation shown by proton emitters is found with the help of the potential energy surface plot.

References

[1] B. Blank, M. J. G. Borge, *Progress in Particle and Nuclear Physics,* **60**, (2008), 403.

[2] C. N. Davids, *Nucl. Phys.,* **A630**, (1998), 321c.

[3] P. J. Sellin, *Phys. Rev.,* **C47**, (1993), 193.

[4] K. P. Rykaczewski, R. K. Grzywacz, M. Karny, J. W. McConnell, Y. M. Momayez, Y. J. Wah, Z. Janas, J. C. Batchelder, C. R. Bingham, D. Hartley, M. N. Tantawy, C. J. Gross, T. N. Ginter, J.H. Hamilton, W. D. Kulp, M. Lipoglavsek, A. Piechaczek, E. F. Zganjar, W.B. Walters, J.A. Winger, *Nucl. Phys.*, **A682**, (2001), 270.

[5] R. D. Page, L. Bianco, I. G. Darby, J. Uusitalo, D. T. Joss, T. Grahn, R. D. Herzberg, J. Pakarinen, J. Thomson, S. Eeckhaudt, P. T. Greenlees, P. M. Jones, R. Julin, S. Juutinen, S. Ketelhut, M. Leino, A. P. Leppanen, M. Nyman, P. Rahkila, J. Saren, C. Scholey, A. Steer, M. B. Gomez, Hornillos, J. S. Al-khalili, P. D. Stevenson, S. Erturk, B. Gall, B. Hadinia, M. Venhart, J. Simpson, *Phys. Rev.,* **C75**, (2007), 061302R.

[6] C. A. Radha, V. Ramasubramanian, E. J. J. Samuel, *Turk. J Phys.,* **34**, (2010), 159.

[7] M. C. Lopes, E. Maglione, L.S. Ferreira, *Physics Letters,* **B673**, (2009), 15.

[8] C. N. Davids, H. Esbensen, *Phys. Rev.,* **C69**, (2004), 034314.

[9] C. N. Davids, P. J. Woods, *Hyperfine Interactions*, **132**, (2001), 133.

[10] J. M. Dong, H. F. Zhang, G. Royer, *Phys. Rev.*, **C79**, (2009), 054330.

[11] S. B. Duarte, O. A. P. Tavares, F. Guzman, A. Dimarco, F. Garcia, O. Rodriguez and M. Goncalves, *Atomic Data and Nuclear Data Tables*, **80**, (2002), 235.

[12] F. Iachello, *Phys. Rev. Lett.*, **92**, (2004), 212501.

[13] G. Shanmugam, Kalpana Sankar, K. Ramamurthi, *Phys. Rev.,* **C52**, (1995), 1443.

[14] G. Shanmugam, B. Kamalaharan, *Phys.Rev.*, **C38**, (1988), 1377.

[15] G. Shanmugam, B. Kamalaharan, *Phys.Rev.*, **C41**, (1990), 1742.

[16] G. Shanmugam, B. Kamalaharan, *Phys.Rev.,* **C41**, (1990), 1184.

[17] M. Ivascu, I. Cata-Danil, D. Bucurescu, G. H. Cata-Danil, L. Stroe, F. Soramel, C. Signorini, A. Guglielmetti, R. Bonetti, *Romanian Reports in Physics*, **57**, (2005), 671.

[18] S. G. Nilsson, I. Ragnarsson, *Shapes and Shells in Nuclear Structure,* (Cambridge, England, Cambridge University Press, 1995).

[19] G. Audi, O. Bersillon, J. Blachot, A. H. Wapstra, *Nucl. Phys.*, **A729**, (2003), 3.

[20] M. Thoennessen, *Phys. Rev.,* **C63**, (2000), 014308.

[21] B. Singh, J. A. Cameron, *Nuclear Data Sheets,* **107,** (2006), 225.

[22] K. Vogt, T. Hartmann, A. Zilges, *Phys. Lett.,* **B517**, (2001), 255.

[23] G. Yuan, D. J. Min, Z. H. Fei, Zuo Wei, Li Jun-Qing, *Chin. Phys.*, **C33**, (2009), 848.

[24] H. Y. Zhang W. Q. Shen, Z. Z. Rent, Y. G. Ma, J. G. Chen, X. Z. Cai, C. Zhong, X. F. Zhou, Y.B. Wei, *Nucl. Phys.*, **A722**, (2003), 518c.

[25] A. Lalazissis D. Vretenar, P. Ring, *Nucl. Phys.*, **A679**, (2001), 481.

[26] L. S. Ferreira, E. Maglione, *Phys. Rev.*, **C61**, (2000), 021304 R.

[27] G. Shanmugam, Carmel Vigila Bai, *PRAMANA-J. Phys.*, **53**, (1999), 457.

[28] T. Vertse A. T. Kruppa, W. Nazarewicz, *Phys. Rev.*, **C61**, (2000), 064317.

[29] J. P. Vivien A. Nourreddine, F. A. Beck, T. Byrski, C. Gehringer, B. Haas, J. C. Merdinger, D. C. Radford, Y. Schutz, J. Dudek, W. Nazarewicz, *Phys. Rev.,* **C33**, (1986), 2007.

[30] W. Nazarewicz J. Dobaczewski, T. R. Werner, J. A. Maruhn, P. G. Reinhard, K. Rutz, C. R. Chinn, A. S. Umar, M. R. Strayer, *Phys. Rev.*, **C53**, (1996), 740.

[31] P. Moller, D. G. Madland, A. J. Sierk, A. Iwamoto, *Nature,* **409**, (2001), 785.

[32] D. Seweryniak, *Nuclear Data Sheets,* **95**, (2002), 1.

[33] P. B. Semmes, *Nucl. Phys.,* **A682**, (2001), 239c.

[34] F. Guzman, M. Gongalves, O. A. P. Tavares, S. B. Duarte, E. Garcia, O. Rodriguez, *Phys. Rev.,* **C59**, (1999), R2339.

[35] K. P. Rykaczewski, *Eur. Phys. J.,* **A15**, (2002), 81.

[36] B. Barmore, A. T. Kruppa, W. Nazarewicz, T. Vertse, Phys. *Rev.,* **C62,** (2000), 054315.

[37] D. S. Delion, R. J. Liotta, R. Wyss, *Physics Reports*, **424**, (2006), 113.